doi: 10.18323/2782-4039-2024-1-67-4

# Special aspects of the microstructure evolution at the temperature-speed deformation of a medical purpose magnesium alloy of the Mg–Zn–Y alloying system



***Kristina K. Kudasheva****, engineer of the Research Institute of Advanced Technologies
***Mikhail L. Linderov***[1], PhD (Physics and Mathematics),
senior researcher of the Research Institute of Advanced Technologies
***Aleksandr I. Brilevskiy***[2], junior researcher
of the Research Institute of Advanced Technologies
***Aleksey V. Danyuk***[3], PhD (Physics and Mathematics),
senior researcher of the Research Institute of Advanced Technologies
***Igor S. Yasnikov***[4], Doctor of Sciences (Physics and Mathematics), Associate Professor,
professor of Chair "General and Theoretical Physics",
leading researcher of the Research Institute of Advanced Technologies
***Dmitry L. Merson***[5], Doctor of Sciences (Physics and Mathematics), Professor,
Director of the Research Institute of Advanced Technologies
*Togliatti State University, Togliatti (Russia)*

***E-mail: a.abdugaffarova@gmail.com**

[1]ORCID: https://orcid.org/0000-0001-8655-4191
[2]ORCID: https://orcid.org/0000-0002-5780-6094
[3]ORCID: https://orcid.org/0000-0002-7352-9947
[4]ORCID: https://orcid.org/0000-0002-6120-7836
[5]ORCID: https://orcid.org/0000-0001-5006-4115

*Received 15.06.2023* *Accepted 26.07.2023*

***Abstract:*** Biocompatibility makes magnesium alloys attractive functional materials in terms of their use as biodegradable implants. However, the technologies for manufacturing semi-finished products carry a possible diversity of the local strain rate and temperature within a rather wide range, which affects the processed material structure and properties. The purpose of this study is to determine the range of temperatures and resistance to deformation, at which there is no negative effect on the main structural characteristics of the processed material, using the example of a medical purposes alloy of the Mg–Zn–Y alloying system. The authors carried out mechanical tests of a biodegradable Mg–1Zn–2.9Y magnesium alloy at various temperatures and strain rates. The influence of temperatures in the range of 20...400 °C on the structure and properties of the Mg–Zn–Y system alloy is disclosed. Starting from a temperature of 350 °C, the process of dynamic recrystallisation is accompanied both by the complete restoration (return) of the original microstructure and by coarsening of the grain size, which can adversely affect the material functional characteristics. The high thermal stability of the biodegradable Mg–1Zn–2.9Y magnesium alloy is revealed, which probably results from the presence of the LPSO phase in it. The study shows that the deformation process is accompanied by twinning. At a strain rate of $2 \cdot 10^{-2}$ $s^{-1}$ over the entire temperature range, the grain size distribution slightly narrows and shifts towards smaller diameters. The application of the obtained results in technological processes for manufacturing medical semi-finished products will help to solve the issue of microstructure instability at the stage of transition from a semi-finished product to a finished product during subsequent thermomechanical treatments.

***Keywords:*** medical purpose magnesium alloys; biodegradable magnesium alloys; Mg–1Zn–2.9Y; temperature-speed deformation; medical purpose alloy; magnesium alloys; dynamic recrystallisation; microstructure evolution.

***Acknowledgements:*** The research is financially supported by the Russian Science Foundation within the scientific project No. 20-19-00585.

The paper was written using the reports of the participants of the XI International School of Physical Materials Science (SPM-2023), Togliatti, September 11–15, 2023.

***For citation:*** Kudasheva K.K., Linderov M.L., Brilevskiy A.I., Danyuk A.V., Yasnikov I.S., Merson D.L. Special aspects of the microstructure evolution at the temperature-speed deformation of a medical purpose magnesium alloy of the Mg–Zn–Y alloying system. *Frontier Materials & Technologies*, 2024, no. 1, pp. 37–47. DOI: 10.18323/2782-4039-2024-1-67-4.

## INTRODUCTION

Recently, biodegradable magnesium alloys have drawn the attention of developers of medical materials due to their attractive properties, including osteointegration [1; 2]. In fact, they formed a separate class of new generation biodegradable metal materials. Compared to other metal materials used as orthopaedic implants, such as titanium, titanium alloys, and stainless steels, the elastic modulus of magnesium alloys is closest in value

to that of human bone tissue [3]. Moreover, magnesium and its alloys are already used as temporary implants that are completely degradable in a biological environment (*in vivo*), and are replaced by newly formed bone, which eliminates the necessity of repeated surgical interference to remove the implant. Many studies have proven that magnesium alloys are safe, and effective materials for medical implants [3–5]. Magnesium ions released from the alloy showed good biological activity [6–8]. The magnesium alloy implanted in the human body is gradually destroyed (dissolved) and absorbed [9], and excess magnesium ions are removed from the human body due to metabolism. The absence of the necessity of repeated operations to remove implants significantly reduces morbidity and the risk of injury. This feature makes them extremely attractive to the market of biodegradable metal implants designed to restore bones that require temporary support.

Despite all the advantages, magnesium and its alloys are characterised by relatively low strength and corrosion resistance. Many studies have been carried out to improve their mechanical properties and corrosion resistance by alloying [10; 11]. For example, the addition of rare-earth metals promotes dynamic recrystallisation of magnesium alloys and increases tensile strength without loss of ductility [12; 13]. The addition of yttrium (Y) can simultaneously improve both ductility [14] and corrosion resistance [15] of a magnesium alloy. Moreover, a significant improvement in the properties of magnesium alloys is possible due to surface modification [16].

At present, much attention is paid to the hardening of magnesium and its alloys by methods based on severe plastic deformation (SPD), in particular, multi-axial isothermal forging [17]. Magnesium and its alloys are poorly deformed, since they have a hexagonal close-packed lattice, and only two primary slip systems: (0001)<1120> and (1010)<1120> [18]. To increase the number of possible slip systems, it is usually necessary to increase the deformation processing temperature, which naturally negatively affects the final properties of the material [19].

The modern technology for manufacturing macroscopic products from magnesium and its alloys is quite well deveoped, however, for most medical products, semi-finished products of small sizes in one or two dimensions (foil, thin-walled tubes, wire, etc.) are required. The manufacture of such semi-finished products is associated with the application of large deformation technologies (drawing, rolling, and extrusion). The development of a technology for the production of medical devices is impossible without knowing the temperature-velocity behaviour of alloys in the process of active deformation. At the same time, the ultimate goal is both to develop a technology for manufacturing thin-walled semi-finished products and to form the required functional properties, which are largely determined by the microstructure characteristics.

Since the microstructure of metals and alloys is formed as a result of dynamic rearrangements of a defective ensemble, and acoustic emission (AE) arising during their deformation is a unique phenomenon capable of precisely reflecting defect dynamics [20], in this work, we will use AE as an experimental method of controlling and diagnosing the evolution of a defective ensemble *in situ*, including for monitoring possible recrystallisation processes.

The purpose of this work is to determine the influence of temperature-velocity factors on possible recrystallisation processes and microstructure parameters of a medical purpose alloy of the Mg–Zn–Y alloying system.

## METHODS

### Material and test samples

To carry out the research, a low alloy with a nominal composition of Mg–1Zn–2.9Y (at. %) was selected, which was manufactured based on Mg95V pig magnesium at SOMZ LLC (Solikamsk).

The chemical composition of the produced alloy was determined using an ARL 4460-1632 high-precision optical emission spectrometer. The results of the chemical composition analysis are shown in Table 1.

End sections containing casting defects were cut off from the resulting castings, and to remove surface defects, the castings were machined on a lathe. After mechanical treatment, the blanks were subjected to homogenising at 430 °C for 24 h.

Multi-axial isothermal forging (MIF) was carried out at the production base of the IMSP RAS (Ufa). When performing each forging cycle, the total degree of deformation ε was about 1.4. MIF was implemented using a PA2638 hydraulic press (630 tf) equipped with a UIShB 510 isothermal die block with flat dies and an induction heater. In total, the blank underwent 16 forging cycles in the temperature range of 325...400 °C. At the final stage, to obtain plates, the blank was upset on a press at 325 °C.

The mechanical properties of the resulting material were evaluated using two types of cylindrical specimens made according to the drawings (Fig. 1). For mass testing, the samples had a working part with a diameter of 5 mm and a length of 25 mm (Fig. 1 a), and for tests with AE registration, the samples were more massive: 8 mm in diameter, 40 mm long, and with a flat for installing an AE sensor (Fig. 1 b). The longitudinal axis of the samples corresponded to the expanding direction (RD) after upsetting.

### Experimental technique

Samples were tested for uniaxial tension on an Instron 8802 universal servohydraulic testing system (England) with nominal strain rates: $5\cdot10^{-4}$, $5\cdot10^{-3}$, $2\cdot10^{-2}$ $s^{-1}$, using an Instron 3119-406 climate chamber at temperatures: 20, 100, 150, 200, 250, 300, and 400 °C (heating uniformity was controlled using thermocouples).

Additional tests were carried out:

1) the alloy in the initial state was kept in a furnace at 400 °C (the holding time was chosen to be equal to the time of testing the sample with a strain rate of $5\cdot10^{-3}$ $s^{-1}$ by 8 %);

2) the alloy in the initial state was deformed by 8 % with a strain rate of $5\cdot10^{-3}$ $s^{-1}$ at room temperature, and then kept in a furnace at 400 °C (the holding time was chosen to be equal to the time of testing the sample with a strain rate of $5\cdot10^{-3}$ $s^{-1}$ by 8 %).

***Table 1.*** *Chemical composition of the Mg–Zn–Y system alloy*
***Таблица 1.*** *Химический состав сплава системы Mg–Zn–Y*

| Name of alloy | Alloying elements, at. % | | | | |
|---|---|---|---|---|---|
| | Mg | Zn | Y | Zr* | Other elements' amount |
| Mg–1Zn–2.9Y | Base | 0.8 | 2.2 | 0.076 | 0.1 |

*Note. *Zirconium is added to a melt to reduce the content of iron impurities and grain refinement.*
*Примечание. *Цирконий добавляется в расплав для снижения содержания примесей железа и измельчения зерна.*

***a*** ***b***

***Fig. 1.*** *Specimens for mechanical tests:* ***a*** *– for mass temperature-speed tests;*
***b*** *– with a flat for tests with simultaneous recording of an acoustic emission signal*
***Рис. 1.*** *Образцы для механических испытаний:* ***a*** *– для массовых температурно-скоростных испытаний;*
***b*** *– с лыской для испытаний с одновременной регистрацией сигнала акустической эмиссии*

Deformation was measured using an Epsilon 3448 extensometer (item 3, Fig. 2).

To record the AE signal, the authors used the equipment consisting of a MSAE-1300WB broadband piezoelectric transducer (Microsensors, Sarov) with an operating frequency range of 50...1300 kHz; a PAC 2/4/6 low-noise preamplifier (USA) with a bandwidth of 10...1200 kHz and an amplification of +60 dB; a PAC PCI-2 low-noise registration system, which allows recording a signal into the computer memory in streaming mode (stream) with a resolution of 16 bits and a signal sampling frequency of 2 MHz, input filter bandwidth of 100...1000 kHz, and additional amplification of +6 dB. After testing, the recorded stream was sequentially divided into frames with a duration of 4096 samples, for each of which the energy (*E*) and median frequency (*fm*) (the frequency dividing the area under the spectral density power curve into two equal parts) were calculated and synchronized with the deformation curve. The AE technique is described in more detail in our earlier work [20].

The microstructure study was carried out on cross-sectional tensile specimens (TD) in the middle of the working base. Microstructure analysis was performed using the EBSD method. The metallographic specimens were prepared by grinding on a sandpaper of different grain sizes, polishing using a diamond suspension (with a particle size ranging from 9 μm to 0.25 μm) and Hitachi IM4000 Plus finishing ion polishing (Japan) (the inclination of 3° to the surface, acceleration of 6 kV and discharge of 1.5 kV, argon gas 0.1 $cm^3$/min and 25 rpm 1–2 h).

To estimate the microstructure parameter, the authors used a Zeiss Sigma scanning electron microscope (Carl Zeiss, Germany) equipped with a TFE cathode and an EDAX/TSL backscattered electron diffraction detector (EDAX, Mahwa, New Jersey, USA). Microstructure scanning was carried out with a step of 250...350 nm, the structural element reliability criterion was 6÷8 points, with a codirectional orientation within 5°. Based on the obtained structure maps, histograms of grain-boundary angles and grain sizes were constructed. The diameter of a circle with an equivalent area was chosen as the grain size estimate.

## RESULTS

The initial microstructure of the Mg–1Zn–2.9Y alloy (Fig. 3 a) consists of fine grains (average diameter is (1.5±0.7) μm) slightly elongated as a result of alloy upsetting after MIF. The grain size distribution is lognormal (Fig. 3 b), and the histogram of grain-boundary angles (Fig. 3 c) reveals a maximum around a 30° angle.

As an example, Fig. 4 shows mechanical diagrams for uniaxial tensile tests of specimens at temperatures of 20 (Fig. 4 a) and 200 °C (Fig. 4 b) with three strain rates.

Due to the fact that the level of AE signals turned out to be very low even at room temperature, it was possible to carry out correct tests only for the highest strain rate ($2\cdot10^{-2}$ $s^{-1}$). As an example, Fig. 5 shows diagrams of the AE parameters combined with the uniaxial tension curve in the test temperature range of 20–250 °C and at a strain rate of $2\cdot10^{-2}$ $s^{-1}$.

At elevated temperatures of mechanical tests, the presented diagrams (Fig. 5 b–d) show a sharp transition to plastic deformation resembling a yield tooth, which is not observed in tests at room temperature. The presence of two kinks is also visible in the diagram. In this interval (from the "yield tooth" to the last "kink"), the deformation is accompanied by a rather powerful AE.

The study of the microstructure in specimens tested at a maximum strain rate of $2\cdot10^{-2}$ $s^{-1}$ at temperatures of 150, 200, 250, and 300 °C was carried out after loading was stopped at a total strain of 4, 8, and 16 %. As an example, a view of the microstructure (Fig. 6 a) is shown, as well as the histograms of grain size distributions (Fig. 6 b) and grain-boundary angles (Fig. 6 c) after tests at a temperature of 250 °C and with a degree of deformation of 16 %.

According to the results of the studies, no significant changes in the structure compared to the initial state (Fig. 3) at all temperatures and degrees of deformation were revealed. The investigated alloy has a high thermal stability, which is probably related to the presence of the LPSO phase in it.

Since no significant changes occurred in the structure in the temperature range of 20–300 °C, to find the boundary of such "insensitivity", it was decided to additionally test the specimens with a strain rate of $5\cdot10^{-3}$ $s^{-1}$ up to a strain of 8 % at 350 and 400 °C. As can be seen, in these cases, the microstructure (Fig. 7, 8) consists of larger grains and the peak in the histogram of distribution of grain boundaries over the grain-boundary angles shifted closer to ~90°.

To identify the reasons for the growth of average grain size, which may be associated with dynamic or static recrystallisation, the authors carried out additional studies. Fig. 9 and 10 show the microstructures of the samples, as well as the grain size distributions and distributions of grain-boundary angles after soaking at 400 °C (Fig. 9) and after soaking at 400 °C of the Mg–1Zn–2.9Y alloy predeformed by 8 % at room temperature with a strain rate of $5\cdot10^{-3}$ $s^{-1}$ (Fig. 10).

## DISCUSSION

At the highest temperature of tests with AE registration (250 °C), the dependence of the median frequency on time (of strain) is of oscillatory character (Fig. 5 d). According to our hypothesis, this may be related to the recrystallisation nature, in particular, to the fact that, the dynamic recrystallisation process in the Mg–1Zn–2.9Y alloy proceeds continuously (does not coincide in time in spatially separated regions of the metal) due to the presence of the LPSO phase in it.

The study of the microstructure in samples tested at a maximum strain rate of $2\cdot10^{-2}$ $s^{-1}$ at temperatures of 150, 200, 250, and 300 °C of testing carried out after the loading was stopped, and at a total strain of 4, 8, and 16 % (Fig. 6) showed no significant changes compared to the initial state (Fig. 3). The investigated alloy has a high thermal stability, which is probably related to the presence of the LPSO phase in it. However, the following peculiarities were identified:

1) in all cases, except for the initial state, the histograms of the grain-boundary angles show a high-angle component (a peak near 90°) associated with twin boundaries (Fig. 6 c), i. e., mechanical twinning was present in all the cases studied;

2) at the highest strain rate at all temperatures, the grain size distribution narrows and shifts towards smaller diameters in relation to the initial state, which has a positive effect on the material functional characteristics.

Comparing the results of action of a temperature of 400 °C on a material in the static state (in the initial (Fig. 9) and deformed by 8 % (Fig. 10) states) with the result of exposure to the same temperature, but in the dynamic mode (at active deformation (Fig. 8)) demonstrates fundamental changes. If in the dynamic mode at a temperature of 400 °C, compared to lower temperatures, the average grain size grows, but at a low grain size nonhomogeneity (Fig. 8 a, 8 b), then in the static mode at a temperature of 400 °C, the process of inhomogeneous recrystallisation occurs with the formation of interlayers of large grains (Fig. 9 a, 9 b), which is even more pronounced after a preliminary deformation of 8 % (Fig. 10 a, 10 b).

Thus, starting from a temperature of 350 °C, the process of dynamic recrystallisation in the alloy under study is accompanied both by the complete restoration (return) of the initial microstructure and by coarsening of the grain size, which can adversely affect the Mg–1Zn–2.9Y alloy functional parameters.

## CONCLUSIONS

Based on the results of mechanical tests of a medical purpose magnesium alloy of the Mg–Zn–Y alloying system, it was found that in the range of test temperature (150÷300) °C and rate ($5\cdot10^{-4}$÷$2\cdot10^{-2}$) $s^{-1}$, no significant changes occur in the structure compared to the initial state (after multi-axial isothermal forging). The investigated alloy has a high thermal stability, which is obviously attributed to the presence of the LPSO phase in it. The formation of a peak near the 90° angle on the histograms of the distribution of grain-boundary angles indicates a significant role of the twinning process in the overall deformation process. Moreover, at the highest strain rate over the entire temperature range, the grain size distribution narrows slightly and shifts towards smaller diameters, which positively affects the Mg–1Zn–2.9Y alloy microstructure and the material functional characteristics.

Starting from a temperature of 350 °C, the process of dynamic recrystallisation is accompanied both by

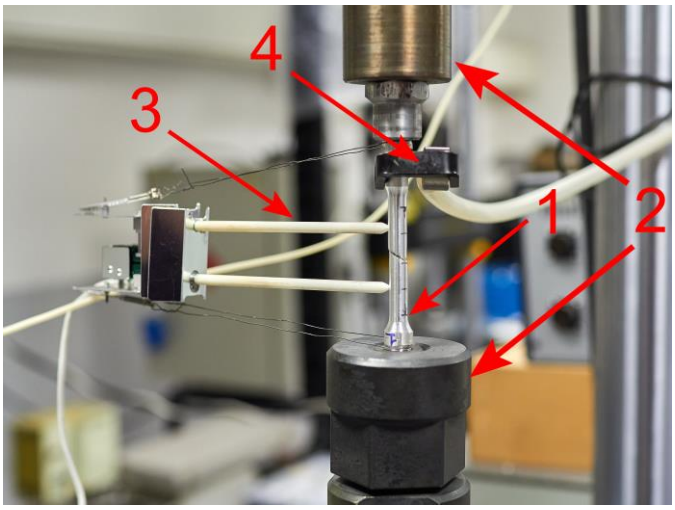


***Fig. 2.*** *A unit for uniaxial tensile tests of specimens:*
*1 – specimen; 2 – jaws; 3 – extensometer; 4 – acoustic emission sensor*
***Рис. 2.*** *Установка для испытаний на одноосное растяжение образцов:*
*1 – образец; 2 – захваты; 3 – экстензометр; 4 – датчик акустической эмиссии*

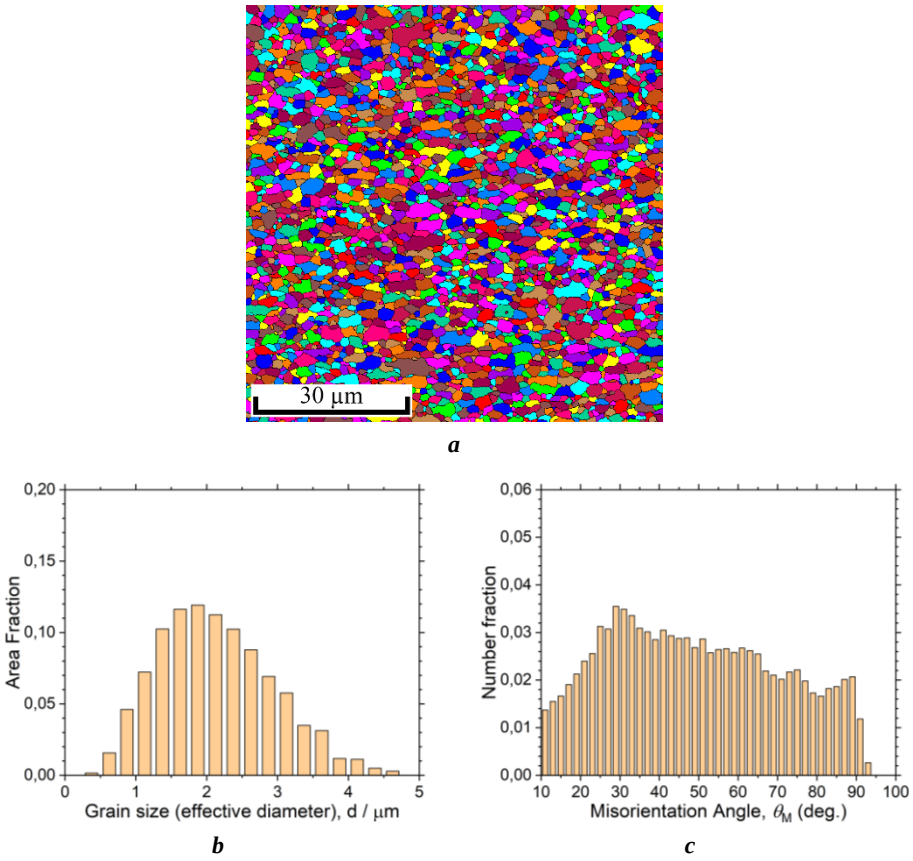


***Fig. 3.*** *Microstructure (**a**), grain size distribution (**b**), and grain-boundary angle distribution (**c**) of the Mg–1Zn–2.9Y alloy in the initial state*
***Рис. 3.*** *Микроструктура (**a**), распределение зерен по размерам (**b**) и распределение по углам разориентировки (**c**) сплава Mg–1Zn–2,9Y в исходном состоянии*

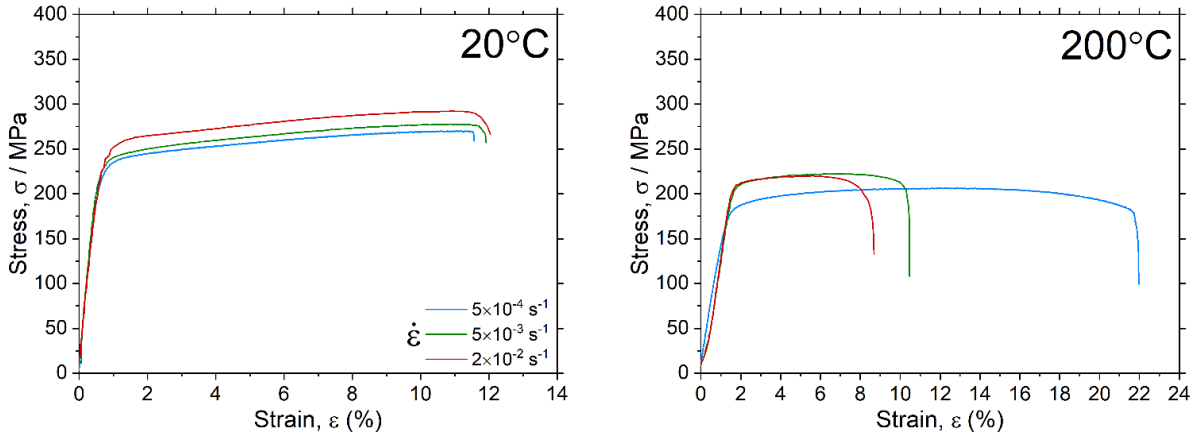


*a* *b*

***Fig. 4.*** *Diagrams of mechanical tests in the "stress – strain" coordinates for three rates of deformation at temperatures of 20 °C (**a**) and 200 °C (**b**)*
***Рис. 4.*** *Диаграммы механических испытаний в координатах «напряжение – деформация» для трех скоростей деформации при температурах 20 °C (**a**) и 200 °C (**b**)*

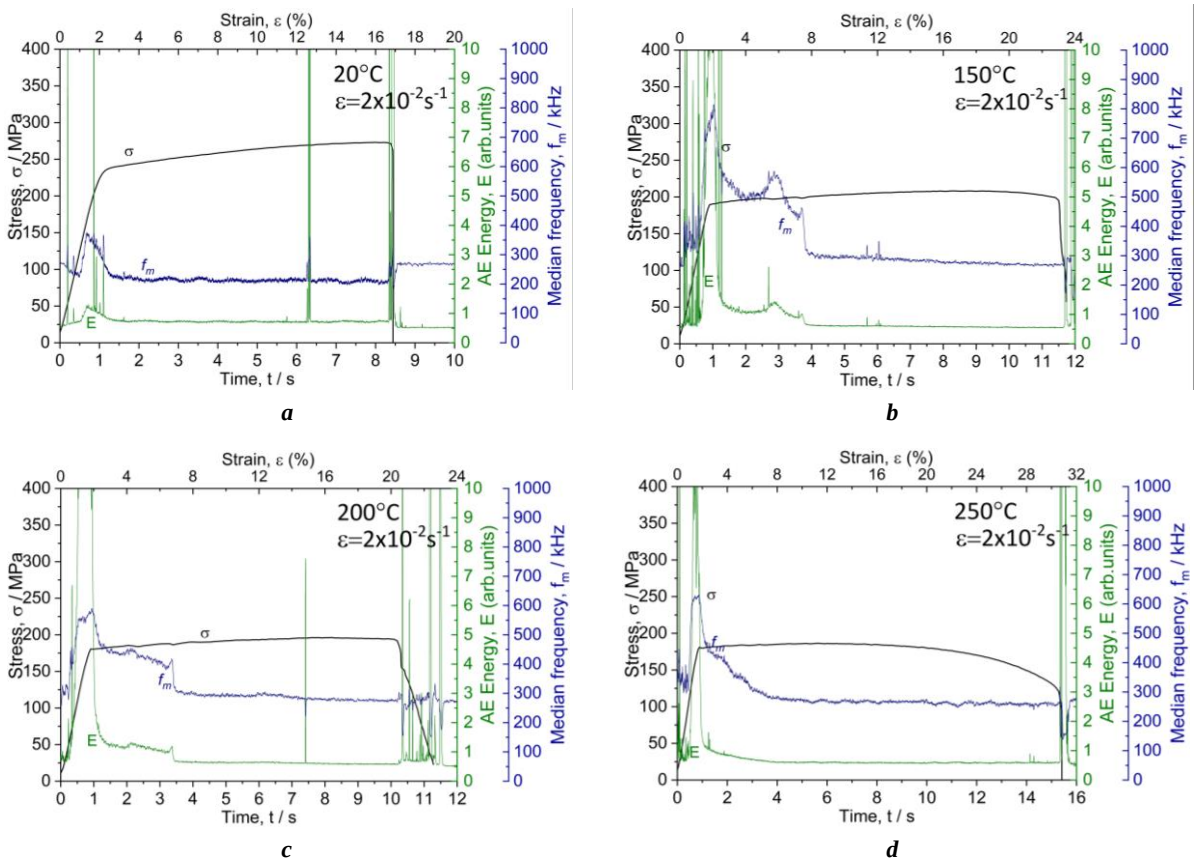


*a* *b*

*c* *d*

***Fig. 5.*** *Diagrams of acoustic emission signal parameters brought in coincidence with the curve of uniaxial tension at test temperatures of 20 °C (**a**), 150 °C (**b**), 200 °C (**c**), and 250 °C (**d**) and deformation rate of $2 \cdot 10^{-2}$ $s^{-1}$*
***Рис. 5.*** *Диаграммы параметров сигнала акустической эмиссии, совмещенные с кривой одноосного растяжения при температурах испытаний 20 °C (**a**), 150 °C (**b**), 200 °C (**c**) и 250 °C (**d**) и скоростью деформирования $2 \cdot 10^{-2}$ $c^{-1}$*

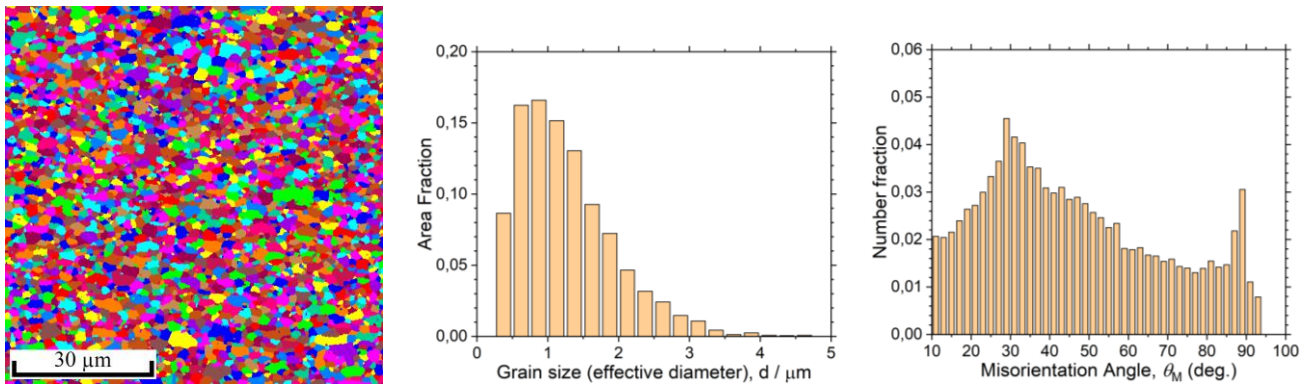


*a* *b* *c*

***Fig. 6.*** *Microstructure (**a**), grain size distribution (**b**), and grain-boundary angle distribution (**c**) of the Mg–1Zn–2.9Y alloy after temperature tests at 250 °C with a deformation rate of $2 \cdot 10^{-2}$ $s^{-1}$ and deformation degree of 16 %*
***Рис. 6.*** *Микроструктура (**a**), распределение зерен по размерам (**b**) и распределение по углам разориентировки (**c**) сплава Mg–1Zn–2,9Y после температурных испытаний при 250 °C со скоростью деформации $2 \cdot 10^{-2}$ $с^{-1}$ и степенью деформации 16 %*

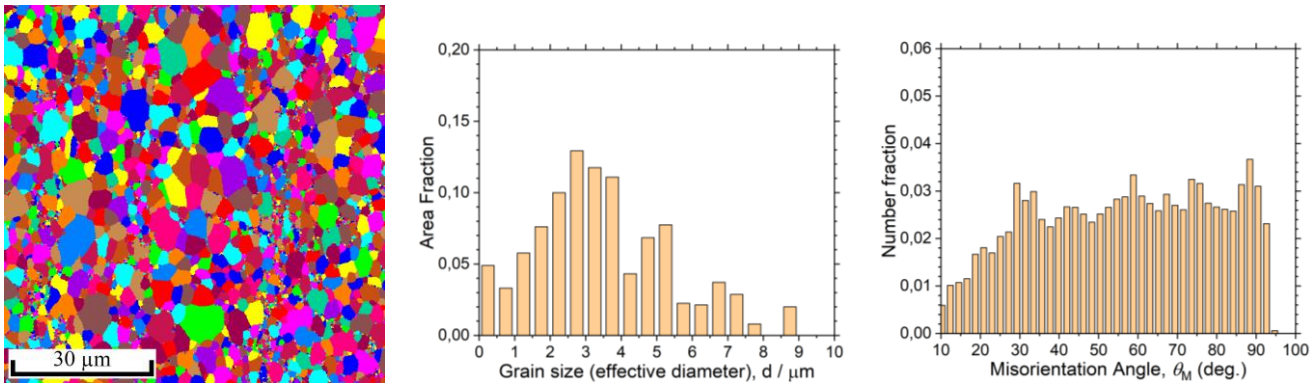


*a* *b* *c*

***Fig. 7.*** *Microstructure (**a**), grain size distribution (**b**), and grain-boundary angle distribution (**c**) of the Mg–1Zn–2.9Y alloy after temperature tests at 350 °C with a deformation rate of $5 \cdot 10^{-3}$ $s^{-1}$ and deformation degree of 8 %*
***Рис. 7.*** *Микроструктура (**a**), распределение зерен по размерам (**b**) и распределение по углам разориентировки (**c**) сплава Mg–1Zn–2,9Y после температурных испытаний при 350 °C со скоростью деформации $5 \cdot 10^{-3}$ $с^{-1}$ и степенью деформации 8 %*

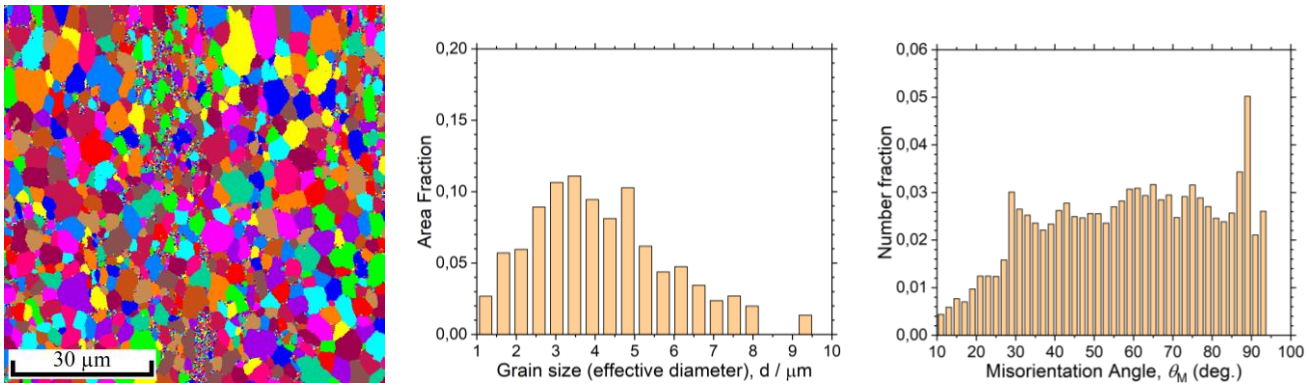


*a* *b* *c*

***Fig. 8.*** *Microstructure (**a**), grain size distribution (**b**), and grain-boundary angle distribution (**c**) of the Mg–1Zn–2.9Y alloy after temperature tests at 400 °C with a deformation rate of $5 \cdot 10^{-3}$ $s^{-1}$ and deformation degree of 8 %*
***Рис. 8.*** *Микроструктура (**a**), распределение зерен по размерам (**b**) и распределение по углам разориентировки (**c**) сплава Mg–1Zn–2,9Y после температурных испытаний при 400 °C со скоростью деформации $5 \cdot 10^{-3}$ $с^{-1}$ и степенью деформации 8 %*

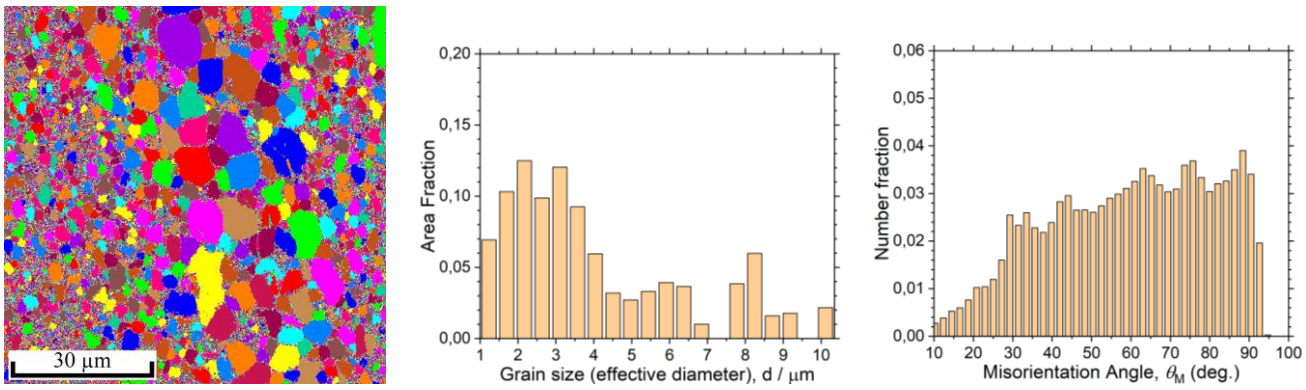


*a* *b* *c*

***Fig. 9.*** *Microstructure (**a**), grain size distribution (**b**), and grain-boundary angle distribution (**c**) of the Mg–1Zn–2.9Y alloy after soaking at a temperature of 400 °C*

***Рис. 9.*** *Микроструктура (**a**), распределение зерен по размерам (**b**) и распределение по углам разориентировки (**c**) сплава Mg–1Zn–2,9Y после выдержки при температуре 400 °C*

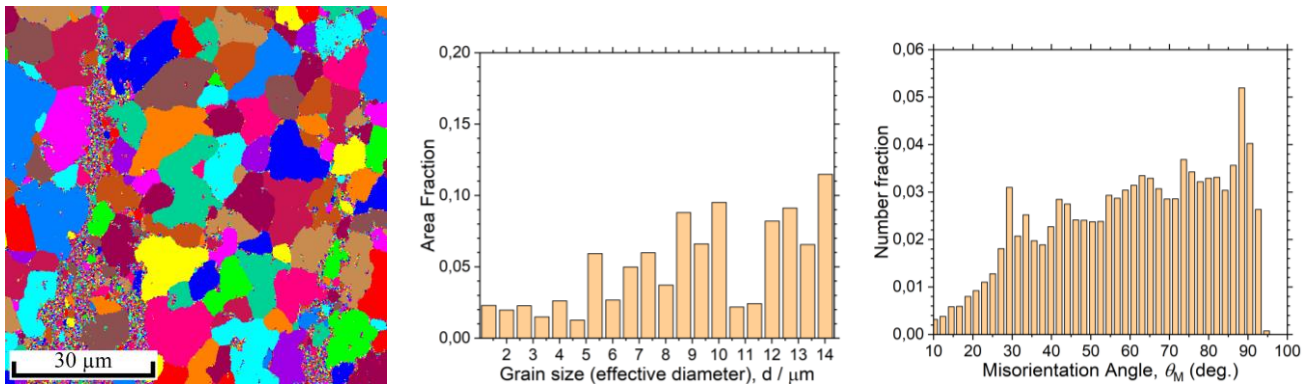


*a* *b* *c*

***Fig. 10.*** *Microstructure (**a**), grain size distribution (**b**), and grain-boundary angle distribution (**c**) of the Mg–1Zn–2.9Y alloy after 8 % deformation at room temperature with a deformation rate of $5 \cdot 10^{-3}$ $s^{-1}$ and further soaking at 400 °C*

***Рис. 10.*** *Микроструктура (**a**), распределение зерен по размерам (**b**) и распределение по углам разориентировки (**c**) сплава Mg–1Zn–2,9Y после деформации 8 % при комнатной температуре со скоростью деформации $5 \cdot 10^{-3}$ $c^{-1}$ и дальнейшей выдержке при 400 °C*

the complete restoration (return) of the original microstructure and by coarsening of the grain size, which can adversely affect the material functional characteristics and is unacceptable with regard to the variability of technological parameters.

Thus, the Mg–1Zn–2.9Y alloy in the state after multiaxial isothermal forging has a thermally stable fine-grained structure, which allows leveling the negative effect of possible fluctuations in the technological parameters of shaping in the range of strain temperature (150÷300) °C and rates $(5 \cdot 10^{-4} \div 2 \cdot 10^{-2})$ $s^{-1}$.

## REFERENCES


1. Prakasam M., Locs J., Salma-Ancane K., Loca D., Largeteau A., Berzina-Cimdina L. Biodegradable materials and metallic implants-A review. *Journal of Functional Biomaterials*, 2017, vol. 8, no. 4, article number 44. DOI: 10.3390/jfb8040044.
2. Li Nan, Zheng Yufeng. Novel Magnesium Alloys Developed for Biomedical Application: A Review. *Journal of Materials Science & Technology*, 2013, vol. 29, no. 6, pp. 489–502. DOI: 10.1016/j.jmst.2013.02.005.
3. Kumar K., Gill R.S., Batra U. Challenges and opportunities for biodegradable magnesium alloy implants. *Materials Technology*, 2018, vol. 33, no. 2, pp. 153–172. DOI: 10.1080/10667857.2017.1377973.
4. Hort N., Huang Y., Fechner D. et al. Magnesium alloys as implant materials – Principles of property design for Mg–RE alloys. *Acta Biomaterialia*, 2010, vol. 6, no. 5, pp. 1714–1725. DOI: 10.1016/j.actbio.2009.09.010.
5. Song Guang-Ling, Song Shizhe. A Possible Biodegradable Magnesium Implant Material. *Advanced Engineering Materials*, 2007, vol. 9, no. 4, pp. 298–302. DOI: 10.1002/adem.200600252.
6. Ali W., Mehboob A., Han Min-Gu, Chang Seung-Hwan. Experimental study on degradation of mechanical properties of biodegradable magnesium alloy (AZ31)

wires/poly(lactic acid) composite for bone fracture healing applications. *Composite Structures*, 2019, vol. 210, pp. 914–921. DOI: 10.1016/j.compstruct.2018.12.011.
7. Bommala V.K., Krishna M.G., Rao C.T. Magnesium matrix composites for biomedical applications: A review. *Journal of Magnesium and Alloys*, 2019, vol. 7, no. 1, pp. 72–79. DOI: 10.1016/j.jma.2018.11.001.
8. Suljevic O., Fischerauer S.F., Weinberg A.M., Sommer N.G. Immunological reaction to magnesium-based implants for orthopedic applications. What do we know so far? A systematic review on in vivo studies. *Materials Today Bio*, 2022, vol. 15, article number 100315. DOI: 10.1016/j.mtbio.2022.100315.
9. Liu Wenwen, Guo Shuo, Tang Zhen, Wei Xinghui, Gao Peng, Wang Ning, Li Xiaokang, Guo Zheng. Magnesium promotes bone formation and angiogenesis by enhancing MC3T3-E1 secretion of PDGF-BB. *Biochemical and Biophysical Research Communications*, 2020, vol. 528, no. 4, pp. 664–670. DOI: 10.1016/j.bbrc.2020.05.113.
10. Xia Yu, Wu Liang, Yao Wen-hui et al. In-situ layered double hydroxides on Mg−Ca alloy: Role of calcium in magnesium alloy. *Transactions of Nonferrous Metals Society of China*, 2021, vol. 31, no. 6, pp. 1612–1627. DOI: 10.1016/S1003-6326(21)65602-9.
11. Dong Jianhui, Lin Tao, Shao Huiping, Wang Hao, Wang Xueting, Song Ke, Li Qianghua. Advances in degradation behaviour of biomedical magnesium alloys: A review. *Journal of Alloys and Compounds*, 2022, vol. 908, article number 164600. DOI: 10.1016/j.jallcom.2022.164600.
12. Chen Junxiu, Kolawole S.K., Wang Jianhua, Su Xuping, Tan Lili, Yang Ke. Systems, Properties, Surface Modification and Applications of Biodegradable Magnesium-Based Alloys: A Review. *Materials*, 2022, vol. 15, no. 14, p. 5031. DOI: 10.3390/ma15145031.
13. Tekumalla S., Seetharaman S., Almajid A., Gupta M. Mechanical Properties of Magnesium-Rare Earth Alloy Systems: A Review. *Metals*, 2015, vol. 5, no. 1, pp. 1–39. DOI: 10.3390/met5010001.
14. Das A.K. Recent trends in laser cladding and alloying on magnesium alloys: A review. *Materials Today: Proceedings*, 2022, vol. 51, part 1, pp. 723–727. DOI: 10.1016/j.matpr.2021.06.217.
15. Gao Jia-cheng, Wu Sha, Qiao Li-ying, Wang Yong. Corrosion behavior of Mg and Mg-Zn alloys in simulated body fluid. *Transactions of Nonferrous Metals Society of China*, 2008, vol. 18, no. 3, pp. 588–592. DOI: 10.1016/S1003-6326(08)60102-8.
16. Jagadeesh G.V., Setti S.G. Surface Modification of Biodegradable Magnesium Alloy by Ball Burnishing Process. *Recent Advances in Materials Technologies: Select Proceedings of ICEMT 2021*. Springer Nature Singapore, 2023, pp. 327–334. DOI: 10.1007/978-981-19-3895-5_26.
17. Figueiredo R.B., Langdon T.G. Achieving Microstructural Refinement in Magnesium Alloys through Severe Plastic Deformation. *Materials Transactions*, 2009, vol. 50, no. 1, pp. 111–116. DOI: 10.2320/matertrans.MD200818.
18. Bryła K., Dutkiewicz J., Lityńska-Dobrzyńska L., Rokhlin L.L., Kurtyka P. Influence of number of ECAP passes on microstructure and mechanical properties of AZ31 magnesium alloy. *Archives of Metallurgy and Materials*, 2012, vol. 57, no. 3, pp. 711–717. DOI: 10.2478/v10172-012-0077-5.
19. Aksenov D.A., Nazarov A.A., Raab G.I., Raab A.G., Fakhretdinova E.I., Asfandiyarov R.N., Shishkunova M.A., Sementeeva Yu.R. Effects of Severe Plastic Deformation and Ultrasonic Treatment on the Structure, Strength, and Corrosion Resistance of Mg–Al–Zn Alloy. *Materials*, 2022, vol. 15, no. 20, p. 7200. DOI: 10.3390/ma15207200.
20. Merson D., Linderov M., Brilevsky A., Danyuk A., Vinogradov A. Monitoring Dynamic Recrystallisation in Bioresorbable Alloy Mg–1Zn–0.2Ca by Means of an In Situ Acoustic Emission Technique. *Materials*, 2022, vol. 15, no. 1, p. 328. DOI: 10.3390/ma15010328.

## СПИСОК ЛИТЕРАТУРЫ

1. Prakasam M., Locs J., Salma-Ancane K., Loca D., Largeteau A., Berzina-Cimdina L. Biodegradable materials and metallic implants-A review // Journal of Functional Biomaterials. 2017. Vol. 8. № 4. Article number 44. DOI: 10.3390/jfb8040044.
2. Li Nan, Zheng Yufeng. Novel Magnesium Alloys Developed for Biomedical Application: A Review // Journal of Materials Science & Technology. 2013. Vol. 29. № 6. P. 489–502. DOI: 10.1016/j.jmst.2013.02.005.
3. Kumar K., Gill R.S., Batra U. Challenges and opportunities for biodegradable magnesium alloy implants // Materials Technology. 2018. Vol. 33. № 2. P. 153–172. DOI: 10.1080/10667857.2017.1377973.
4. Hort N., Huang Y., Fechner D. et al. Magnesium alloys as implant materials – Principles of property design for Mg–RE alloys // Acta Biomaterialia. 2010. Vol. 6. № 5. P. 1714–1725. DOI: 10.1016/j.actbio.2009.09.010.
5. Song Guang-Ling, Song Shizhe. A Possible Biodegradable Magnesium Implant Material // Advanced Engineering Materials. 2007. Vol. 9. № 4. P. 298–302. DOI: 10.1002/adem.200600252.
6. Ali W., Mehboob A., Han Min-Gu, Chang Seung-Hwan. Experimental study on degradation of mechanical properties of biodegradable magnesium alloy (AZ31) wires/poly(lactic acid) composite for bone fracture healing applications // Composite Structures. 2019. Vol. 210. P. 914–921. DOI: 10.1016/j.compstruct.2018.12.011.
7. Bommala V.K., Krishna M.G., Rao C.T. Magnesium matrix composites for biomedical applications: A review // Journal of Magnesium and Alloys. 2019. Vol. 7. № 1. P. 72–79. DOI: 10.1016/j.jma.2018.11.001.
8. Suljevic O., Fischerauer S.F., Weinberg A.M., Sommer N.G. Immunological reaction to magnesium-based implants for orthopedic applications. What do we know so far? A systematic review on in vivo studies // Materials Today Bio. 2022. Vol. 15. Article number 100315. DOI: 10.1016/j.mtbio.2022.100315.
9. Liu Wenwen, Guo Shuo, Tang Zhen, Wei Xinghui, Gao Peng, Wang Ning, Li Xiaokang, Guo Zheng. Magnesium promotes bone formation and angiogenesis by enhancing MC3T3-E1 secretion of PDGF-BB // Biochemical and Biophysical Research Communications. 2020. Vol. 528. № 4. P. 664–670. DOI: 10.1016/j.bbrc.2020.05.113.

10. Xia Yu, Wu Liang, Yao Wen-hui et al. In-situ layered double hydroxides on Mg−Ca alloy: Role of calcium in magnesium alloy // Transactions of Nonferrous Metals Society of China. 2021. Vol. 31. № 6. P. 1612–1627. DOI: 10.1016/S1003-6326(21)65602-9.
11. Dong Jianhui, Lin Tao, Shao Huiping, Wang Hao, Wang Xueting, Song Ke, Li Qianghua. Advances in degradation behavior of biomedical magnesium alloys: A review // Journal of Alloys and Compounds. 2022. Vol. 908. Article number 164600. DOI: 10.1016/j.jallcom.2022.164600.
12. Chen Junxiu, Kolawole S.K., Wang Jianhua, Su Xuping, Tan Lili, Yang Ke. Systems, Properties, Surface Modification and Applications of Biodegradable Magnesium-Based Alloys: A Review // Materials. 2022. Vol. 15. № 14. P. 5031. DOI: 10.3390/ma15145031.
13. Tekumalla S., Seetharaman S., Almajid A., Gupta M. Mechanical Properties of Magnesium-Rare Earth Alloy Systems: A Review // Metals. 2015. Vol. 5. № 1. P. 1–39. DOI: 10.3390/met5010001.
14. Das A.K. Recent trends in laser cladding and alloying on magnesium alloys: A review // Materials Today: Proceedings. 2022. Vol. 51. Part 1. P. 723–727. DOI: 10.1016/j.matpr.2021.06.217.
15. Gao Jia-cheng, Wu Sha, Qiao Li-ying, Wang Yong. Corrosion behavior of Mg and Mg-Zn alloys in simulated body fluid // Transactions of Nonferrous Metals Society of China. 2008. Vol. 18. № 3. P. 588–592. DOI: 10.1016/S1003-6326(08)60102-8.
16. Jagadeesh G.V., Setti S.G. Surface Modification of Biodegradable Magnesium Alloy by Ball Burnishing Process // Recent Advances in Materials Technologies: Select Proceedings of ICEMT 2021. Singapore: Springer Nature Singapore, 2023. P. 327–334. DOI: 10.1007/978-981-19-3895-5_26.
17. Figueiredo R.B., Langdon T.G. Achieving Microstructural Refinement in Magnesium Alloys through Severe Plastic Deformation // Materials Transactions. 2009. Vol. 50. № 1. P. 111–116. DOI: 10.2320/matertrans.MD200818.
18. Bryła K., Dutkiewicz J., Lityńska-Dobrzyńska L., Rokhlin L.L., Kurtyka P. Influence of number of ECAP passes on microstructure and mechanical properties of AZ31 magnesium alloy // Archives of Metallurgy and Materials. 2012. Vol. 57. № 3. P. 711–717. DOI: 10.2478/v10172-012-0077-5.
19. Aksenov D.A., Nazarov A.A., Raab G.I., Raab A.G., Fakhretdinova E.I., Asfandiyarov R.N., Shishkunova M.A., Sementeeva Yu.R. Effects of Severe Plastic Deformation and Ultrasonic Treatment on the Structure, Strength, and Corrosion Resistance of Mg–Al–Zn Alloy // Materials. 2022. Vol. 15. № 20. P. 7200. DOI: 10.3390/ma15207200.
20. Merson D., Linderov M., Brilevsky A., Danyuk A., Vinogradov A. Monitoring Dynamic Recrystallisation in Bioresorbable Alloy Mg–1Zn–0.2Ca by Means of an In Situ Acoustic Emission Technique // Materials. 2022. Vol. 15. № 1. P. 328. DOI: 10.3390/ma15010328.

# Особенности эволюции микроструктуры при температурно-скоростном деформировании магниевого сплава медицинского назначения системы легирования Mg–Zn–Y



***Кудашева Кристина Камильевна****, инженер НИИ прогрессивных технологий
***Линдеров Михаил Леонидович***[1], кандидат физико-математических наук,
старший научный сотрудник НИИ прогрессивных технологий
***Брилевский Александр Игоревич***[2], младший научный сотрудник НИИ прогрессивных технологий
***Данюк Алексей Валериевич***[3], кандидат физико-математических наук,
старший научный сотрудник НИИ прогрессивных технологий
***Ясников Игорь Станиславович***[4], доктор физико-математических наук, доцент,
профессор кафедры «Общая и теоретическая физика»,
ведущий научный сотрудник НИИ прогрессивных технологий
***Мерсон Дмитрий Львович***[5], доктор физико-математических наук, профессор,
директор НИИ прогрессивных технологий
*Тольяттинский государственный университет, Тольятти (Россия)*

***E-mail: a.abdugaffarova@gmail.com**

[1]ORCID: https://orcid.org/0000-0001-8655-4191
[2]ORCID: https://orcid.org/0000-0002-5780-6094
[3]ORCID: https://orcid.org/0000-0002-7352-9947
[4]ORCID: https://orcid.org/0000-0002-6120-7836
[5]ORCID: https://orcid.org/0000-0001-5006-4115

*Поступила в редакцию 15.06.2023* *Принята к публикации 26.07.2023*

***Аннотация:*** Биосовместимость делает сплавы магния привлекательными функциональными материалами с точки зрения их использования в качестве биорезорбируемых имплантатов. Однако технологии изготовления полуфабрикатов несут в себе возможное варьирование локальной скорости деформации и температуры в достаточно широком диапазоне, что сказывается на структуре и свойствах обрабатываемого материала. Цель исследования состоит в определении диапазона температур и стойкостей деформации, при которых не происходит

отрицательного влияния на основные структурные характеристики обрабатываемого материала, на примере сплава медицинского назначения системы легирования Mg–Zn–Y. Проведены механические испытания биоразлагаемого магниевого сплава Mg–1Zn–2,9Y при различных температурах и скоростях деформации. Раскрыто влияние температур в диапазоне 20…400 °C на структуру и свойства сплава системы Mg–Zn–Y. Начиная с температуры 350 °C, процесс динамической рекристаллизации сопровождается не только полным восстановлением (возвратом) исходной микроструктуры, но и укрупнением размеров зерна, что может негативно сказаться на функциональных характеристиках материала. Выявлена высокая термостабильность биоразлагаемого магниевого сплава Mg–1Zn–2,9Y, что, вероятно, объясняется наличием в нем LPSO-фазы. Показано, что деформационный процесс сопровождается двойникованием. При скорости деформации $2 \cdot 10^{-2}$ $с^{-1}$ во всем температурном диапазоне распределение зерен по размерам несколько сужается и смещается в сторону меньших диаметров. Использование полученных результатов в технологических процессах изготовления полуфабрикатов медицинского назначения поможет решить проблему нестабильности микроструктуры на стадии перехода от полуфабриката в изделие при последующих термомеханических обработках.

***Ключевые слова:*** магниевые сплавы медицинского назначения; биоразлагаемые магниевые сплавы; Mg–1Zn–2,9Y; температурно-скоростная деформация; сплав медицинского назначения; магниевые сплавы; динамическая рекристаллизация; эволюция микроструктуры.

***Благодарности:*** Исследование выполнено при финансовой поддержке Российского научного фонда в рамках реализации научного проекта № 20-19-00585.

Статья подготовлена по материалам докладов участников XI Международной школы «Физическое материаловедение» (ШФМ-2023), Тольятти, 11–15 сентября 2023 года.

***Для цитирования:*** Кудашева К.К., Линдеров М.Л., Брилевский А.И., Данюк А.В., Ясников И.С., Мерсон Д.Л. Особенности эволюции микроструктуры при температурно-скоростном деформировании магниевого сплава медицинского назначения системы легирования Mg–Zn–Y // Frontier Materials & Technologies. 2024. № 1. С. 37–47. DOI: 10.18323/2782-4039-2024-1-67-4.